ChemSusChem

Research Article
doi.org/10.1002/cssc.202202122

Chemistry Europe
European Chemical
Societies Publishing

www.chemsuschem.org

Integrating Carbohydrate and C1 Utilization for Chemicals Production

Vivian Pascal Willers,[a] Barbara Beer,[a, b] and Volker Sieber*[a, c, d]

In the face of increasing mobility and energy demand, as well as the mitigation of climate change, the development of sustainable and environmentally friendly alternatives to fossil fuels will be one of the most important tasks facing humankind in the coming years. In order to initiate the transition from a petroleum-based economy to a new, greener future, biofuels and synthetic fuels have great potential as they can be adapted to already common processes. Thereby, especially synthetic fuels from CO_2 and renewable energies are seen as the next big step for a sustainable and ecological life. In our study, we directly address the sustainable production of the most common biofuel, ethanol, and the highly interesting next-generation biofuel, isobutanol, from methanol and xylose, which are directly derivable from CO_2 and lignocellulosic waste streams, respectively, such integrating synthetic fuel and biofuel production. After enzyme and reaction optimization, we succeeded in producing either $3\,g\,L^{-1}$ ethanol or $2\,g\,L^{-1}$ isobutanol from $7.5\,g\,L^{-1}$ xylose and $1.6\,g\,L^{-1}$ methanol. In our cell-free enzyme system, C1-compounds are efficiently combined and fixed by the key enzyme transketolase and converted to the intermediate pyruvate. This opens the way for a hybrid production of biofuels, platform chemicals and fine chemicals from CO_2 and lignocellulosic waste streams as alternative to conventional routes depending solely either on CO_2 or sugars.

Introduction

In the face of climate change, depletion of fossil resources, and increasing energy demand, alternative, sustainable energy sources are in demand to replace traditional energy production methods while reducing waste and greenhouse gases such as carbon dioxide (CO_2). One major step will be the replacement of fossil fuels by green electricity, hydrogen or renewable and sustainable biofuels. Here biocatalysis comes into play, which is considered as a green and sustainable technology.[1] Traditional, first-generation biofuel production relies on production from edible crops,[2] but due to food versus fuel debates, this approach needs alternative solutions.[3] Lignocellulosic biomass has high potential as feedstock for the production of biofuels and platform chemicals. It is cheap, economically friendly and ethically acceptable because it is not competing with the food supply.[4] Moreover, in the year 2018 lignocellulosic biomass has been the most abundantly available bio resource with a global yield of up to 1.3 billion tons per year.[5]

However, efficient utilization of residual biomass with an advantageous solution for biofuel production includes the perspective of efficiently converting most of the sugars it contains to the same product.[6] In addition to glucose, xylose with a share of up to 30 to 40% of carbohydrate content in lignocellulose must also be taken into account and used for the production of biofuels.[7] One major drawback in biofuel production using xylose as substrate is that it's not readily utilized by microorganisms.[8] For the two most studied micro-organisms *Saccharomyces cerevisiae* and *Escherichia coli*, growth on xylose is limited[9] and biofuel production based on xylose is only possible by non-conventional or engineered strains. However, titers are not comparable to glucose derived titers. In addition, the production comes with low efficiency and high production cost.[8a] Besides, one major drawback which comes up for the utilization of glucose and xylose using micro-organisms is catabolite repression, i.e., glucose actively represses the expression of genes for xylose transporters and xylose conversion making a co-fermentation of glucose and xylose difficult.[10]

Ethanol as one of the most common and widely used biofuels by now,[11] is naturally produced by many organisms like yeast or bacteria, by conversion of the central metabolite pyruvate.[12] Bioethanol production is mostly based on sugar-cane production by fermentation of glucose with established hosts such as Saccharomyces cerevisiae, which use their natural utilization pathways for ethanol production.[13] In addition, potential waste streams such as crude glycerol expand the possibilities for ethanol production.[14] To produce ethanol from xylose, xylose is first metabolized via xylose isomerase, xylose

[a] V. P. Willers, Dr. B. Beer, Prof. Dr. V. Sieber
     Chair of Chemistry of Biogenic Resources
     Technical University of Munich
     Campus Straubing, 94315 Straubing (Germany)
     E-mail: Sieber@tum.de
[b] Dr. B. Beer
     Current address:
     CASCAT GmbH
     94315 Straubing (Germany)
[c] Prof. Dr. V. Sieber
     Technical University of Munich
     94315 Straubing (Germany)
[d] Prof. Dr. V. Sieber
     School of Chemistry and Molecular Biosciences
     The University of Queensland
     St. Lucia 4072 (Australia)

ChemSusChem

Research Article
doi.org/10.1002/cssc.202202122

Chemistry Europe
European Chemical
Societies Publishing

reductase,xylose dehydrogenase or the Dahms pathway, which leads to the pentose phosphate pathway, or directly to pyruvate.[15] In this process, a maximum of 1.66 molecules of ethanol are formed from one molecule of xylose.[16] Whereas the production of ethanol from xylose is implemented in different microorganisms like *Zymomonas mobilis* or *Saccharomyces cerevisiae* with titers of 43.1 g L^{-1} (0.45 g g^{-1} xylose) and 16.4 g L^{-1} (0.41 g g^{-1} xylose) respectively,[8a] isobutanol production from xylose is rare.

Isobutanol is considered as next-generation biofuel, as well as commodity chemical and has great advantages considering energy density and physicochemical properties compared to ethanol.[17] Isobutanol can also be produced from pyruvate in five steps via acetolactate synthase (AlsS), ketol-acid reductoisomerase (IlvC), dihydroxy-acid dehydratase (IlvD), alpha-keto-acid decarboxylase (KDC) and alcohol dehydrogenase (ADH).[18] If only xylose is used for the production of isobutanol, one molecule of xylose yields at maximum 0.83 molecules of isobutanol.[19]

Glucose, the most abundant sugar in lignocellulose, is efficiently transformed to isobutanol with yields up to 22 g L^{-1} (86% theoretical yield between 40 h and 112 h) in a time range of 112 h, using *E. coli*[20] or with different cell free system with yields up to 275 g L^{-1}.[18,21] In contrast, the conversion of xylose suffers from low product titers, with 92.9 mg L^{-1}.[22] The highest titer of isobutanol so far was reached by Zhang et al. using xylose and *S. cerevisiae* strain Yzy197 in a fed batch approach to produce 3.1 g L^{-1} in 192 h (maximum daily theoretical yield of 9.4%) in a mixed approach for the production of branched-chain higher alcohols.[23] This demonstrates that there is room for improvement and need for it as the long fermentation time and low efficiency prohibitive. Accordingly, in order to produce biofuels sustainably and economically from lignocellulosic biomass and as basic requirement to replace chemical synthesis for isobutanol involving high temperatures and pressures,[24] rapid and efficient utilization of xylose is necessary.[15]

Whereas xylose assimilation pathways mostly rely on cleavage of xylose to a C3 and a C2 precursor molecule, which is either rearranged for example in the pentose phosphate pathway or directly used for the production of various chemicals like ethylene glycol, acetoin or glycolic acid.[25] C1 assimilation pathways can link the cleavage of a sugar to the fixation of a CO$_2$ based C1-compound.[26] One example of this pathway is the naturally occurring xylulose monophosphate pathway found in methylotrophic yeast.[27] Here xylulose 5-phosphate is cleaved together with formaldehyde into glyceraldehyde 3-phosphate and dihydroxyacetone by dihydroxyacetone synthase. These C3 precursors are then rearranged and every cycle of fixation produces 0.33 molecules of pyruvate from one C1-compound.[28] By combining the pyruvate generated from xylose and CO$_2$, one molecule of isobutanol or two molecules of ethanol can be produced from one molecule of xylose and CO$_2$. The strategy of using methanol as the C1-compound and a second carbon compound as xylose or gluconate was shown recently.[29] Here for example, methanol-auxotrophic *E. coli* strains were developed as proof-of-concept, in which ethanol or a mixture of ethanol and 1-butanol were

obtained from the redesigned ribulose-5-phosphate pathway. However, only 43% of the produced ethanol and 71% of 1-butanol contained carbon derived from methanol.[29a]

In addition to whole-cell systems, *in vitro* systems have recently become increasingly important because they are becoming more complex and offer the possibility of producing various compounds from cheap substrates with high efficiency. Furthermore, these synthetic cascades based on purified enzymes have many advantages. They have high controllability, adaptability, manipulatable reaction conditions, easy product recovery, and higher tolerance to toxic substances.[30] Moreover, the suppression of carbon catabolism mentioned above does not occur, and the separation of products such as isobutanol can be easily performed by using approaches with a two-phase system.[21]

The immersive potential to integrate C1-compounds in enzymatic cascades was shown by Cai et al., who set up a multi-enzymatic cascade for the production of starch from CO$_2$-based methanol.[31] Isobutanol production based on CO$_2$ was shown *in vivo* as proof of concept by Atsumi et al. with a final titer of 0.45 g L^{-1} by using cyanobacteria.[32] The highest titer of isobutanol from CO$_2$ was reached by Miao et al. producing 0.9 g L^{-1} in a time span of 40 days.[33] However, no *in vitro* pathway using CO$_2$ for the production of isobutanol was shown before. Guo et al. proposed a pathway from CO$_2$ to isobutyraldehyde by combining the carbon-carbon bond forming modules from Cai et al. with a glycolysis module to form pyruvate and from pyruvate a third module to isobutyraldehyde, but lacked experimental proof.[34] In this way, isobutanol could be produced exclusively from C1-chemicals, but the key enzyme formolase, which produces dihydroxyacetone from formaldehyde, lacks high activity and specificity for formaldehyde. Large amounts of expensive protein would be required to produce isobutyraldehyde or isobutanol.

Inspired by the intriguing possibilities of using green C1-chemicals, that are derived directly from CO$_2$ using green energy/hydrogen, as building blocks for the production of sustainable carbon compounds, coupled with the challenging use of the C5 sugar xylose from lignocellulosic biomass waste, we developed an artificial enzymatic xylose-based C1 fixation and utilization pathway (XFUP). This pathway allows the efficient use of CO$_2$-derived C1-compounds using xylose to produce ethanol and isobutanol. With the need for new pathways to produce biofuels and commodity chemicals with lower environmental burden, the optimized XFUP enables highly efficient production of isobutanol in a minimum time span at low temperatures, and with non-toxic solvents. In a proof of concept 8.5 mM isobutanol could be obtained from 10 mM xylose and formaldehyde corresponding to 85% theoretical yield in 12 h. Furthermore, adaptation of the system to methanol leads to a final titer of either 3 g L^{-1} ethanol or 2 g L^{-1} isobutanol in 24 h.

ChemSusChem

Research Article
doi.org/10.1002/cssc.202202122

**Chemistry
Europe**
European Chemical
Societies Publishing

Results and Discussion

Implementation of a sugar-guided CO₂ fixation pathway to biofuels

For the production of ethanol and isobutanol from C1-precursors with xylose, we built up a modular cascade, consisting of a C1 fixation module, a cofactor regeneration module as well as a biofuel production module, which is adaptable, to produce either ethanol or isobutanol (Scheme 1).

The C1 fixation module is based on the xylulose mono-phosphate pathway consuming xylose and formaldehyde with the key enzyme transketolase (TktA). Here, xylose is isomerized by xylose isomerase (XylA) and directly utilized by transketolase with the fixation of formaldehyde to produce glyceraldehyde and dihydroxyacetone. Dihydroxyacetone and glyceraldehyde are then phosphorylated by a dual active dihydroxyacetone kinase (DhaK) by producing two molecules of ADP. Naturally, xylulose is phosphorylated first by xylulokinase and its product xylulose-5-phosphate is utilized by dihydroxyacetone synthase to produce dihydroxyacetone and glyceraldehyde-3-phosphate

by assimilation of formaldehyde. However, the ability of transketolase to utilize xylulose directly together with the dual active dihydroxyacetone kinase circumvents a possible negative interaction between xylulokinase and dihydroxyacetone kinase due to an imbalanced ATP/ADP concentration and reduces the number of enzymes of the module.

The sugar guided fixation of CO_2 via C1 metabolites provides an efficient alternative to the newly developed formolase based fixation pathway,[35] where three formaldehyde molecules can build up one molecule of pyruvate. The key enzyme in this pathway, formolase, represents the bridge between C1 metabolism and C3 precursor molecules present in glycolysis by coupling three formaldehyde molecules to one dihydroxyacetone. Besides the ingenuity of this reaction, it is also the biggest bottleneck of the pathway, due to the unfavorable kinetic properties of the until now best formolase variant fls-M3 to formaldehyde with a k_{cat} of 0.2 s⁻¹ and a K_m of 23.6 mM.[31] To avoid the accumulation of high toxic concentrations of formaldehyde, which inactivate enzymes and inhibit the growth of microorganisms, high concentrations of formolase are required, which is not economically feasible in up-
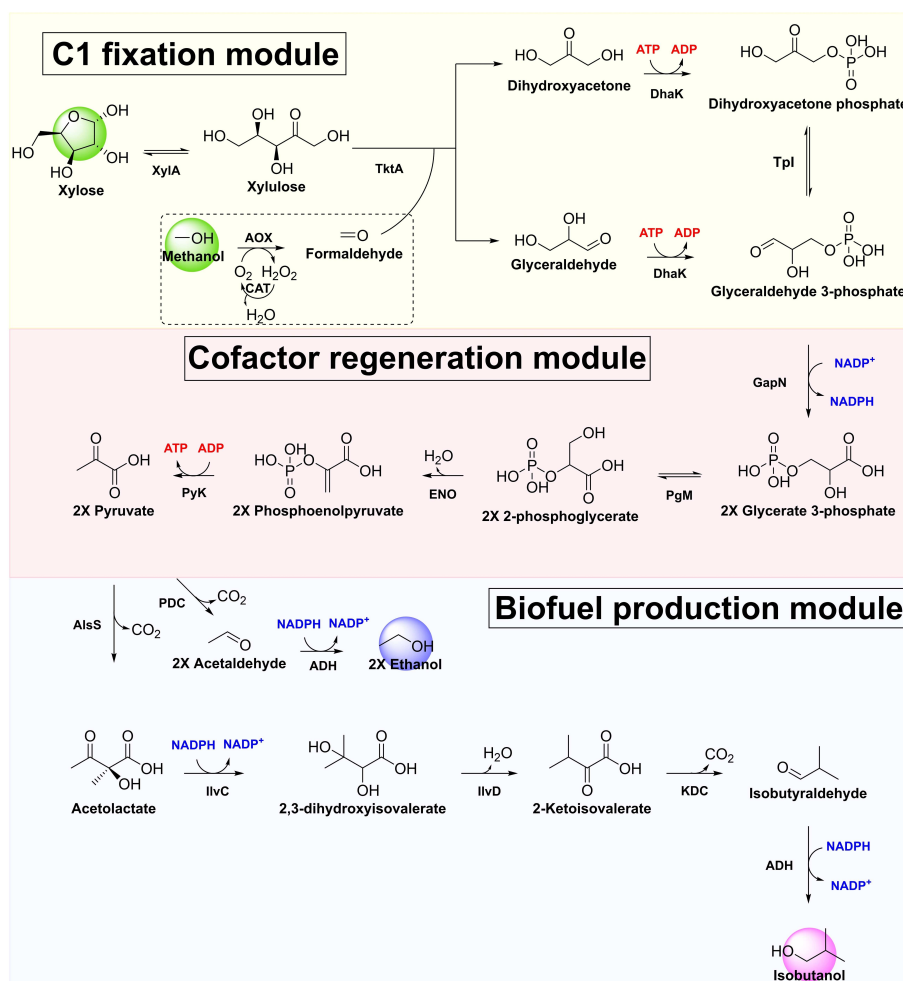
Scheme 1. Schematic representation of modular cascade with ATP (blue) and NADP⁺ (red) regeneration system including enzymes, substrates, intermediates and final products. Yellow highlighted alternative methanol entry point to the cascade.

ChemSusChem

Research Article
doi.org/10.1002/cssc.202202122

Chemistry Europe
European Chemical
Societies Publishing

scaling approaches. In contrast, the class of transketolases and dihydroxyacetone synthases that occur naturally in sugar-directed formaldehyde fixation pathways could provide an alternative due to their advantageous kinetic properties (e.g., K_m of DhaS of Candida Boindii on formaldehyde 1.0 mM and v_{max} of 4.9 U mg^{-1} in a reaction with xylulose 5-phosphate).[36]

The cofactor regeneration module is based on the lower glycolysis and provides pyruvate as precursor and platform intermediate for the production of ethanol and isobutanol as well as the regeneration of NADPH and ATP. Key enzymes here are pyruvate kinase (PyK), which regenerates ATP by producing pyruvate and a non-phosphorylating NADP$^+$ dependent glyceraldehyde 3-phosphate dehydrogenase (GapN) to balance ATP consumption as well as NADPH recycling.[37]

Finally, the cascade finishes with a biofuel production module that either is based on the natural valine pathway for the production of isobutanol by pyruvate or on the natural ethanol pathway for the production of ethanol from pyruvate. For ethanol production pyruvate is decarboxylated by pyruvate decarboxylase (PDC) and emerging acetaldehyde is further reduced by an NADPH dependent ADH. For the production of isobutanol AlsS combines two pyruvates to acetolactate. Acetolactate is further processed via the natural valine pathway enzymes to 2-ketoisovalerate by producing one molecule of NADP$^+$. 2-Ketoisovalerate is then decarboxylated by KDC and reduced by the NADPH dependent ADH from the ethanol pathway. To drive the reaction, both, the cofactor regeneration module as well as the biofuel production module start with a nearly irreversible reaction (aldehyde dehydrogenase and keto-acid decarboxylase, resp.).

Characterization of key enzymes of XFUP

Transketolase

With the xylose guided fixation and valorization of C1-compounds as the major advantage of the cascade, we first characterized three transketolases (TktA) from the microorganisms *Escherichia coli* (ecTktA), *Variovorax paradoxus* (vpTktA) and *Meiothermus ruber* (mrTktA) for their activity on formaldehyde and xylulose (Figure S2). By comparing the kinetic properties of these with a fixed formaldehyde concentration of 5 mM (Table 1) a range of values of catalytic efficiency from 0.3 to 0.6 [s^{-1} mM^{-1}] was observed. The highest activity was observed for ecTktA with 8 U mg^{-1}. However, affinity of ecTktA for xylulose was low (K_m: 15.9 mM). In contrast to that, activity of mrTktA was the lowest with 1.3 U mg^{-1}, nevertheless it had the highest

affinity for xylulose with 6.4 mM. For the best transketolase ecTktA kinetics were also measured with a fixed concentration of 50 mM xylulose. Here a high affinity was observed with a K_m of 2.1 mM to formaldehyde (Figure S2). However, when different concentrations of formaldehyde were applied on the other transketolases, inhibition occurred at formaldehyde concentrations above 10 mM whereby the strongest inhibition was observed for mrTktA with a 50% reduced activity with 20 mM formaldehyde (Figure S3). When transeketolase and formolase are compared, it is noticeable that the catalytic efficiency of all tested transketolases in the presence of 5 mM formaldehyde is at least one order of magnitude higher, and in the case of ecTktA more than 1.5 orders of magnitude higher than the catalytic efficiency of the formolase-formose reaction. Due to its low catalytic efficiency, future applications of formolase with high substrate loading are not yet possible. Transketolases, with their high activity even at low formaldehyde concentrations, could be an interesting alternative for the use and utilization of CO$_2$-derived formaldehyde. In conjunction, it could serve as a better starting point for an engineering campaign to become industrially attractive.

Dihydroxyacetone kinase

Because the reaction of transketolase with xylulose and formaldehyde yields glyceraldehyde and dihydroxyacetone, phosphorylation of both intermediates is essential to connect the artificial xylulose monophosphate pathway with the lower glycolysis (Figure S4 and Table S2). Dihydroxyacetone kinase from *Kozakia baliensis* (kbDhaK) has a very high affinity for dihydroxyacetone (K_m: 86 ± 30 μM), making it the perfect target for phosphorylation of dihydroxyacetone in the cascade. Surprisingly, we observed activity on glyceraldehyde as substrate in a similar range, with a lower affinity than dihydroxyacetone (K_m: 364.9 ± 32.0 μM). Nevertheless, the affinity is in the μM range and with this dual activity of kbDhaK it is possible to ensure a rapid transfer from the C1 fixation module to lower glycolysis.

Alcohol dehydrogenase

In addition to the unnatural reaction of ecTktA and kbDhaK, the promiscuity of ADH plays a key role in the composition of the cascade. Therefore, a major goal in the selection of alcohol-producing ADH is to minimize its ability to convert formaldehyde in the cascade. As a consequence, we screened three ADHs of *Escherichia coli*[38] on isobutyraldehyde and formaldehyde conversion (Figure S5 and Table S3). ADH ecYahK commonly used in isobutanol production[37,39] due to its high affinity (K_m of 0.2 ± 0.0 mM) and moderate activity of 2.2 ± 0.3 U mg^{-1} is also able to reduce formaldehyde to methanol with a K_m of 6.1 ± 1.4 mM to formaldehyde and an activity of 1.9 ± 0.2 U mg^{-1} in a similar range as for isobutyraldehyde. ADH ecYqhD has a high affinity for isobutyraldehyde (K_m: 2.3 ± 0.3 mM) but a very low affinity for formaldehyde (K_m: 53.4 ±

Table 1. Kinetic parameters of different transketolases with xylulose (0–100 mM) at a fixed formaldehyde concentration of 5 mM (n = 3).

Transketolase	K_m [mM]	v_{max} [U mg^{-1}]	k_{cat} [s^{-1}]	Efficiency [s^{-1} mM^{-1}]
ecTktA	15.9 ± 0.3	8.2 ± 0.1	10.0 ± 0.2	0.6
vpTktA	9.2 ± 0.3	3.1 ± 0.1	4.0 ± 0.1	0.4
mrTktA	6.4 ± 0.1	1.3 ± 0.0	1.6 ± 0.0	0.3

8.6 mM). However, the activity on both substrates is similarly low with 0.2 ± 0.0 U mg^{-1}. ADH ecYjgB has a very low affinity for isobutyraldehyde (K_m: >100 mM) and formaldehyde (K_m: >100 mM). Because of that ecYjgB was not considered further for application in the cascade.

By comparing ecYqhD and ecYahK, ecYahK seems promising as its catalytic efficiency for isobutyraldehyde is more than 50 times higher than for formaldehyde. In contrast to that ecYqhD catalytic efficiency for isobutyraldehyde is only 26 times as high as for formaldehyde (Table S3). However, when we investigated the activity of ADHs on glyceraldehyde, which is also an intermediate in the cascade, ecYahK exhibited 24-fold higher activity than ecYqhD (Figure S6). Due to this site activity and the fact that the formaldehyde concentration in the cascade is kept low, the low activity of ecYqhD on formaldehyde and the low activity on glyceraldehyde were decisive to use ecYqhD as ADH for the cascade. Nevertheless, the low activity of ecYqhD with isobutyraldehyde could cause a bottleneck in the cascade and affect the overall flux, since ADH is part of the NADP$^+$/NADPH regeneration system. Therefore, ecYqhD could be a target for a future engineering approach to strengthen the selectivity and activity of the enzyme.

XFUP assembly and first optimization

Defining the overall cascade set up

Because the cascade assembles 13 enzymes, a quick but efficient thermofluor based stability assay was set up. With this assay the effect of different buffer systems in a pH range of 7.0 to 8.0 on the melting temperature of the cascade enzymes was analyzed (Figure 1a). We speculated that a reduced thermal stability shows a negative influence of the buffer on XFUP and contrary a raised thermal stability a beneficial influence on XFUP.

The highest difference in melting temperature caused by the buffer system showed the GapN of *Thermococcus kodakar-* *ensis* (tkGapN) with a decrease in melting temperature of around 10 °C from >99 °C in tris(hydroxymethyl)aminomethan (TRIS) buffer and 4-(2-hydroxyethyl)-1-piperazineethanesulfonic acid (HEPES) buffer to 90 °C in potassium phosphate (KPi) buffer. Another example for a decrease in melting temperature due to the buffer system is ecYqhD. Similar to tkGapN, ecYqhD melting temperature decreases from 50 °C in HEPES and TRIS buffer to 42 °C in KPi buffer. In contrast, the melting temperature of triosephosphate isomerase of *Geobacillus stearothermophilus* (gsTpI) increases from 74 °C in HEPES and TRIS buffer to 78 °C in KPi buffer. By comparing HEPES and TRIS buffer we detected smaller changes in melting temperature. While dihydroxy-acid dehydratase of *Schlegelella thermodepolymerans* (stIlvD) has a melting temperature of 70 °C in HEPES pH 8.0, this melting temperature drops to 66 °C in TRIS pH 8.0. Contrary, a thermostable variant of *Lactoccocus lactis* KDC (llKDC_7 M.D),[40] has a melting temperature of 75 °C in HEPES pH 7.0 but a melting temperature of 76 °C in TRIS pH 7.0.

The pH of the buffer also changes the melting temperature of the different enzymes. While *Bacillus subtilis* AlsS (bsAlsS) and llKDC_7 M.D show a melting temperature of 62 °C and 75 °C in HEPES at pH 7.0, respectively, those two enzymes have a decreased melting temperature of 60 °C and 69 °C in HEPES, at pH 8.0. These findings are in accordance with the analysis of the pH range for llKDC of Wei et al., which reported an optimal pH of 6.0 to 7.0.[41] Also a decrease in melting temperature of bsAlsS at high pH is in accordance with the pH profile of bsAlsS recorded by Sommer et al., which show that bsAlsS has a pH optimum at pH 6.0.[42] Vice versa, xylose isomerase of *Pseudomonas fluorescens* (pfXylA) and *Geobacillus stearothermophilus* ketol-acid reductoisomerase (gsIlvC) melting temperatures increase from 63 °C and 85 °C in HEPES pH 7.0 to 68 °C and 89 °C in HEPES pH 8.0, respectively.
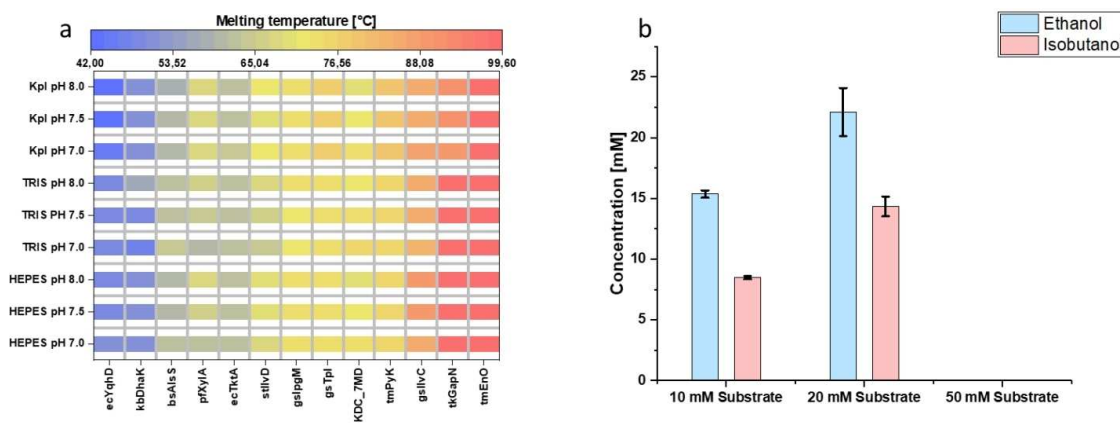
Figure 1. Cascade optimization and initial biofuel production. (a) Thermofluor screening with melting temperature of isobutanol cascade enzymes in three different buffer systems with pH 7.5. (b) Resulting isobutanol and ethanol concentrations after buffer optimization in TRIS pH 7.5 after 12 h of incubation for isobutanol and 16 h incubation for ethanol (n=3).

ChemSusChem

Research Article
doi.org/10.1002/cssc.202202122

**Chemistry
Europe**
European Chemical
Societies Publishing

Cascade assembly and biofuel production

Summarizing the thermofluor results, a more acidic pH of 7.0 and a more basic pH of 8.0 lead to stronger changes in the melting temperature of the enzymes to higher but also to lower values than a neutral pH of 7.5. To not imbalance the cascade by providing a pH which might aid one enzyme but harms others, we chose a pH of 7.5 for initial experiments. By analyzing the buffer systems at pH 7.5 we could also see strong differences between the different enzymes. We speculated that HEPES buffer might be the most constant one because all enzymes showed an intermediate melting temperature. However, to verify how changes in thermal stability observed by thermofluor analysis due to the buffer system can be adapted to the performance of the cascade, we conducted three cascades with different buffer systems (HEPES, TRIS, KPi) at pH 7.5 and 37 °C for the production of isobutanol with 10 mM xylose and formaldehyde as starting substrates (Figure S7).

To ensure rapid conversion of formaldehyde, we chose high concentrations of enzymes from the first module resulting in a similar unit amount of 150 mU (Table S4 and Table S5), measured with low substrate concentrations (Table S2). To further drive the transketolase reaction and provide rapid ATP regeneration, enzyme units from module two were increased by more than three times the units of transketolase. The final enzyme units of module three were similar to those of module one, while KDC and ADH had half the units of module one. Here a lower amount of units were chosen due to a possible site activity of ADH on formaldehyde and glyceraldehyde. As control, we conducted the cascade without transketolase.

By applying these conditions, the cascade with potassium phosphate as buffer system shows the lowest performance. After 12 h, 5.0 ± 0.2 mM isobutanol was formed corresponding to a theoretical yield of 50%. Similarly, in the system with HEPES buffer. Here, 5.6 ± 0.5 mM isobutanol corresponding to 56% theoretical yield was produced in 12 h. The best performance was obtained using a system with TRIS buffer. After 12 h, 8.5 ± 0.1 mM isobutanol (Figure 1b) was built up corresponding to 85% theoretical yield. No isobutanol was built without the addition of transketolase.

To investigate the effect of the toxic formaldehyde together with the buffer system, we doubled the xylose and formaldehyde concentrations to 20 mM (Figure S7). This time the buffer effect increased, with the system with TRIS producing 14.3 ± 0.8 mM isobutanol after 12 h (Figure 1b). The system buffered with potassium phosphate produced only 5.5 ± 0.5 mM isobutanol and the system buffered with HEPES produced 9.2 ± 0.3 mM isobutanol. When the substrate concentration was further increased to 50 mM xylose and formaldehyde, isobutanol could no longer be detected and the enzymes precipitated.

To show the flexibility of the cascade, we used the optimized buffer conditions (TRIS pH 7.5) to produce ethanol as an alternative biofuel (Figure 1b). Therefore, the core of the cascade was not changed and only bsAlsS, gsIlvC, stIlvD and llKDC_7 M.D were switched to PDC of Zymomonas mobilis (zmPDC).[18] At 10 mM, 20 mM, and 50 mM xylose and

formaldehyde, 75%, 55%, and 0% theoretical yield ethanol could be produced, respectively (Figure 1b).

With these initial experiments, a foundation was laid and three statements could be made to address these findings. First, the cascade design performed well and the adaptability of the cascade for the production of isobutanol or ethanol could be efficiently realized. Second, the results of the thermofluor analysis were consistent with the output of the cascade, however not HEPES but TRIS pH 7.5 was the most suitable buffer system. Third, the upscaling of the substrates xylose and formaldehyde from 10 mM to 20 mM could increase the total yield of isobutanol and ethanol significantly from 8.5 mM isobutanol to 14.3 mM isobutanol and from 15 mM ethanol to 22 mM ethanol. Nevertheless, the efficiency of the cascade in production was reduced. In addition to that, an increase from 20 mM to 50 mM xylose and formaldehyde completely inactivates the cascade, whereby no isobutanol or ethanol could be detected. However, these concentrations are already well above the tolerance of Escherichia. coli to formaldehyde, with even a low concentration of 1.5 mM severely impairing cell growth.[43]

Since formaldehyde is a highly reactive and toxic compound, these results highlight the dramatic effects of high formaldehyde concentrations on enzymatic cascades. We suggest that the lower efficiency of the cascade at 20 mM substrate already indicates formaldehyde inactivation, which is exacerbated by even higher concentrations. To overcome this obstacle and realize larger scale *in vitro* systems with integrated C1 fixation up to a future vision of industrial scale, enzymes need to be stabilized either by protein engineering or enzyme immobilization to tolerate higher formaldehyde concentrations.

Optimizing the cascade performance in presence of formaldehyde

As an alternative solution to the problem of high concentrations of toxic formaldehyde, we decided to titrate formaldehyde into the system.

As first option, we used micro syringe pumps to slowly add formaldehyde to the cascade. For this, formaldehyde had a concentration of 100 mM and the flow rate was adjusted to $20 \, \mu L \, h^{-1}$ and $10 \, \mu L \, h^{-1}$ respectively. We applied 50 mM xylose as starting substrate. With this rate, we expected to have equimolar concentrations of xylose and formaldehyde after five hours (ten hours). After five hours (ten hours), we stopped formaldehyde supply and let the cascade run further to see whether it converts the residual formaldehyde and xylose into isobutanol over time (Figure S8). In this setup, formaldehyde solution was pumped into the system via syringes. A major disadvantage of this setup was that the additional formaldehyde diluted the preparation. In addition, it could not be ruled out that the pump pulses were not completely accurate and uniform and thus partial high formaldehyde concentrations could occur during runtime.

In the setting with a formaldehyde supply of $20 \, \mu L \, h^{-1}$, isobutanol was rapidly produced with an initial rate of $5.2 \, mM \, h^{-1}$. However, this rate also rapidly declined after two

ChemSusChem

Research Article
doi.org/10.1002/cssc.202202122

Chemistry Europe
European Chemical
Societies Publishing

hours and nearly no isobutanol was produced afterwards. After seven hours a maximum of 10.5 ± 1.2 mM isobutanol was produced. In contrast to that, isobutanol production in the setting with $10 \, \mu L \, h^{-1}$ formaldehyde supply was slower with an initial rate of 1.7 mM h^{-1}. This time, however, the rate remained constant for four hours, and only then, it decreased rapidly. A total of 7.3 ± 1.7 mM isobutanol was produced after ten hours. The microsyringe approach achieved an initial conversion of xylose and formaldehyde, in contrast to the direct application of 50 mM formaldehyde. However, this approach was not very efficient and isobutanol production quickly came to a halt. By measuring the formaldehyde concentration formaldehyde strongly increased after six hours ($10 \, \mu L \, h^{-1}$ approach) and after three hours respectively ($20 \, \mu L \, h^{-1}$ approach). This strong increase with simultaneous stagnation of isobutanol production could give a hint for enzyme inactivation at this point. In addition, the formaldehyde concentration increased faster than expected, which could be a result of inaccuracy of the microsyringe pumps. Nevertheless, the slower titration of formaldehyde prolonged the production of isobutanol, but again, isobutanol production ends after four hours, and titers are comparable to those of the higher rate titration.

As a more promising alternative to direct formaldehyde titration, we next used methanol as an alternative starting substrate. For this, we added alcohol oxidase and catalase to the system and re-run the cascade with methanol, a less denaturing but similarly important C1-compound that can be obtained directly from CO_2.[44,45] Under the same conditions as before, we were able to generate 26.6 ± 1.8 mM isobutanol from 50 mM xylose and methanol after 24 h of incubation (Figure 2a). A control without the addition of transketolase and methanol oxidase lead to no isobutanol production (Figure S9).

Again, the adaptability of the cell-free system was demonstrated. By adding zmPDC instead of the enzymes for the artificial valine pathway, we switched the system to produce ethanol from xylose and methanol. Using 50 mM xylose and methanol, we were able to produce 66.0 ± 4.5 mM ethanol after six hours (Figure 2b).

These results show that effective prevention of high formaldehyde concentration is the crucial step to operate the system and achieve scalable production of the final products ethanol and isobutanol. However, when looking at the consumption rates of methanol and xylose, there is a sharp decrease directly after the first 30 minutes of runtime. This sharp decrease clearly indicates oxygen limitation in the system. As oxygen has a low solubility in aqueous solutions[46] and the K_m for oxygen of alcohol oxidase of *Pichia pastoris* (ppAOX) is between 0.4 and 1 mM in presence of methanol,[47] reaction rates quickly decline if not actively forcing oxygen into the system. However, this oxygen limitation could also be a reason why the cascade works more efficiently with methanol than when formaldehyde is added with a syringe pump. The slower rate gives the transketolase more time to consume formaldehyde which does not lead to partially high concentrations.

Apart from this, stability of ppAOX could be a reason for the diminished methanol consumption, due to quick loss in activity at elevated temperatures.[47] Because of that future application needs to first address the oxygen affinity by enzyme engineering approaches to keep the oxygen consumption rate high over a certain time span and process engineering to introduce oxygen in an efficient manner without compromising enzyme stability.[48] In addition, oxidase stability could also be a key issue to address, either by lower temperature or more stable oxidases. The final issue that would be needed for scale-up is an engineering of ADH. The ADH still suffers from a low activity towards isobutyraldehyde and to get enough velocity in the cascade, the converting ADH has to be highly active and specific for isobutyraldehyde.

Conclusion

The efficient use of CO_2-based C1-compounds will be one of the greatest opportunities for biocatalysis in the coming years. There are more and more concepts for new enzymes that are able to convert methanol, formaldehyde or formate directly into molecules with higher carbon chain length. However, these pathways pass through the highly reactive and toxic compound formaldehyde, which can deactivate and crosslink enzymes.
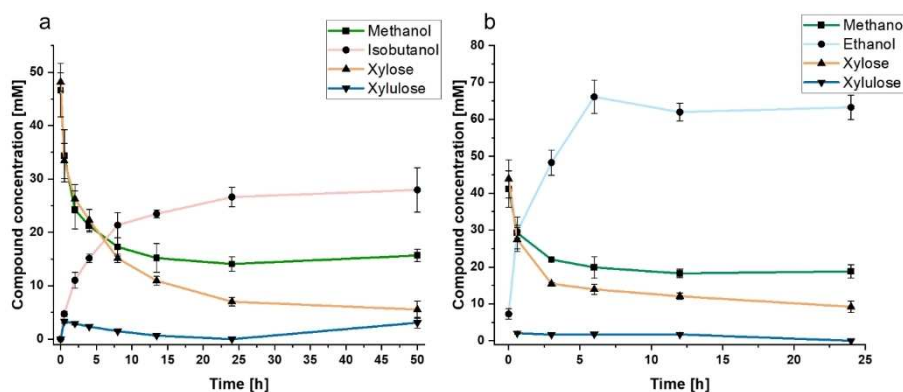
Figure 2. Time course of substrate, product and intermediates of the final cascade. (a) Isobutanol set up with methanol and xylose as substrates. (b) Ethanol set up with methanol and xylose as substrates (n = 3).

ChemSusChem

Research Article
doi.org/10.1002/cssc.202202122

Chemistry Europe
European Chemical
Societies Publishing

Therefore, control over formaldehyde concentration is essential to create sustainable and scalable pathways for industrial application. By exploiting the adaptability of *in vitro* systems, we were able to prevent high formaldehyde concentrations and inactivation of pathway enzymes by the in-situ production of formaldehyde via methanol. In combination with sugar-directed utilization of formaldehyde via transketolase, accumulating formaldehyde is directly converted into key intermediates of glycolysis, which can then be further utilized via pyruvate to generate isobutanol, ethanol or other chemicals.

Using xylose, the second most abundant sugar in nature and after glucose the main carbohydrate of lignocellulosic biomass, and methanol, a C1-compound derivable from CO_2, we have developed a cell-free system for sustainable and efficient production of the most common biofuel ethanol and the highly interesting next-generation biofuel isobutanol with titers of $3\,g\,L^{-1}$ ethanol and $2\,g\,L^{-1}$ isobutanol from $7.5\,g\,L^{-1}$ xylose and $1.6\,g\,L^{-1}$ methanol, respectively. As an alternative to C1-only pathways, xylose-based C1 fixation and utilization pathway (XFUP) fixes formaldehyde using xylose with an active transketolase, preventing interference of high partial formaldehyde concentrations. In addition, the modular design of the cascade allows rapid addition or modification of modules. Thus, in future research and application, a combination of xylose valorization with the already known glucose-isobutanol pathway is possible and both sugars can be converted simultaneously without the problem of catabolite repression. Thus, sugar-guided C1 fixation efficiently combines two waste streams and opens the way for environmentally and economically friendly production of biofuels and chemical feedstocks from waste materials.

Experimental Section

Chemicals and strains

All chemicals were purchased from Sigma-Aldrich, Roth, Alfa Aesar, Merck, Cayman chemical, Carbosynth, Serva, Fisher scientific and VWR unless otherwise noted.

Escherichia coli (E. coli) NEB® Turbo cells (New England Biolabs® inc.) were used as cloning strain. E. coli BL21(DE3) F– ompT gal dcm lon hsdSB(rB- mB-) λ(DE3 [lacI lacUV5-T7 gene 1 ind1 sam7 nin5]) (Novagen) were used for heterologous gene expression.

Pyruvate kinase/Lactate dehydrogenase mix (PK/LDH) from rabbit muscle, alcohol oxidase (AOX) of *Pichia pastoris*, catalase (CAT) of *Corynebacterium glutamicum*, glyceraldehyde 3-phosphate dehydrogenase (GAPDH) from rabbit muscle and aldolase from rabbit muscle were purchased from Sigma-Aldrich. Lactate dehydrogenase (LDH) from rabbit muscle was purchased from Roth.

Molecular cloning and plasmid construction

Plasmid pET28a was provided by Novagen. pCBRHisN, pCBRHisC were constructed on the basis of pET28a and prepared as published by Guterl et al.[18] Phusion High-Fidelity DNA Polymerase (NEB) was used for gene amplification from genomic DNA. Restriction enzymes and T4 ligase (NEB) were used for restriction ligation cloning of plasmids and genes (Table S1).

Protein expression

E. coli BL21(DE3) was used as host strain for heterologous gene expression. Expression was carried out in two steps. First 20 mL of lysogeny broth (LBmedium containing $100\,\mu g\,mL^{-1}$ kanamycin were inoculated with a colony from the LB agar plate and incubated for 16 h at 37 °C and 150 rpm. Main cultures were cultivated in shaking flasks containing 20 % (v v^{-1}) ZYP-5052 auto induction medium[49] including $100\,\mu g\,mL^{-1}$ kanamycin. The main culture was inoculated to an OD_{600} of 0.05 and incubated at 37 °C and 90 rpm until an OD_{600} of 0.6–0.8. Temperature was reduced to 25 °C for enzymes derived from thermophilic organisms and to 16 °C for enzymes derived from mesophilic organisms and incubated for 20 h. Cells were harvested by centrifugation (20 °C, 3500 g, 30 min), the supernatant was discarded and the cell pellet was stored at −20 °C.

Protein purification

Cell lysates were prepared on ice using ultra sonication (Ultraschallprozessor UIS250 V Hielscher Ultrasonic GmbH) and centrifuged afterwards (20 °C, 18000 g, 30 min). For enzymes originated from thermophilic organisms an additional heat treatment was applied before centrifugation (65 °C, 45 min).

Proteins containing a His_6-tag were purified using an AEKTA Pure system equipped with a 5 mL HiTrapFF Crude column. First, the column was equilibrated with binding buffer (50 mM HEPES pH 8.0, 20 mM imidazole, 500 mM NaCl). Then the supernatant was applied. A washing step with binding buffer was used to remove unbound proteins. To elute the His_6-taged proteins from the column, the imidazole concentration was raised from 20 mM to 500 mM. The eluate was fractionated and protein-containing fractions were collected. The buffer was exchanged via HiPrep 26/10 desalting column to 50 mM HEPES pH 7.5. Purified protein solutions were frozen in liquid nitrogen and stored at −80 °C.

Protein concentration determination

Protein concentration was determined using a NanoPhotometer® P-Class (IMPLEN). Absorption was measured at 280 nm after adding extinction coefficient and molecular weight of the target enzyme to the system (Table S1).

Enzyme activity assay

Enzyme activity measurements were conducted in 200 μL reactions with HEPES pH 7.5 and 10 mM $MgCl_2$ at 37 °C. Conditions were tailored according to the analyzed enzymes and coupling enzymes. Reactions were started by addition of the target enzyme and measured by Biotek epoch-2 microplate spectrophotometer (Biorad) (Table S2).

ATP depended reactions were coupled to pyruvate kinase and lactate dehydrogenase with the use of phosphoenolpyruvate as co-substrate. Activity was measured by following the absorbance of NADH at 340 nm.

NAD(P)$^+$/NAD(P)H depended reactions were directly measured by following the absorbance of NAD(P)H at 340 nm.

All other reactions were coupled to ATP depended reactions and monitored as described for ATP dependent reactions or coupled to NAD(P)$^+$ or NAD(P)H consuming reactions by following the absorbance of NAD(P)H at 340 nm

Enzyme kinetic measures

Transketolase

Transketolase (TktA) kinetics (Figure S2) were measured in a coupled approach with glyceraldehyde specific aldehyde dehydrogenase taAldH (M42)[50] by measuring reduction of NAD$^+$. To test whether M42 activity is reduced by formaldehyde, activity of M42 was tested on glyceraldehyde by measuring the reduction of NAD$^+$ in presence of 0 to 20 mM formaldehyde (Figure S3). Due to formaldehyde inactivation, M42 concentration was raised four times in kinetic measurements to counteract reduced activity in high formaldehyde concentrations.

Xylulose kinetics were conducted with a concentration range of 0 to 100 mM of xylulose and a fixed concertation of 5 mM formaldehyde. Reaction was started by addition of xylulose to the reaction mixture. Formaldehyde kinetics were conducted with a concentration range of 0 to 20 mM of formaldehyde and a fixed concentration of 50 mM xylulose. Reaction was started by addition of formaldehyde to the reaction mixture

Formaldehyde inhibition of vpTktA and mrTktA (Figure S3) was measured similar to the kinetics with formaldehyde. Here, a fixed concentration of 5 mM xylulose was applied. However, to counteract the inhibition of the coupling enzyme, M42 concentration was increased fourfold. Reaction was started by addition of formaldehyde to the reaction mixture.

Dihydroxyacetone kinase

Dihydroxyacetone kinase (DhaK) kinetics (Figure S4) were measured in a coupled approach with pyruvate kinase and lactate dehydrogenase by measuring oxidation of NADH[51] in 382 μL. Standard reactions contained additional 1.25 mM PEP, 0.3 mM NADH, 2 mM ADP, 5 to 0.005 mM dihydroxyacetone and 3.8 μL Pyk/LDH mix. Reactions were started by addition of dihydroxyacetone to the reaction mixture.

Alcohol dehydrogenase

Alcohol dehydrogenase (ADH) kinetics (Figure S5) were measured by directly measuring the oxidation of NADPH.[38] Standard reaction contained additional 0.3 mM NADPH and 0 to 50 mM isobutyraldehyde or 0 to 250 mM formaldehyde. Reaction was started by addition of the substrate to the reaction mixture.

Melting point analysis

Melting point analysis was performed in 25 μL reaction volume with 2 μL SYPRO™ Orange (1:80 dilution) 2 μL of protein (concentration), and 100 mM TRIS pH 7.5, HEPES pH 7.5 or KpI pH 7.5 in the cascade matrix. Measurements were performed with a CFX96 Touch Real-Time PCR detection system (Biorad). The temperature was increased in increments of 1 °C from 25 °C to 100 °C with one minute per kelvin increase. The melting curves were prepared as described in the manufacturer's instructions (Biorad). Melting point data were derived from the minimum of the negative derivative of the fluorescence curve versus temperature (Biorad).

Enzymatic cascade

Enzymatic cascades for the production of ethanol and isobutanol were conducted as follows. The enzymes were concentrated and desalted with a buffer changed to the cascade buffer using modified PES 10 kDa (VWR) centrifugal filters.

Initial cascade with buffer test and formaldehyde as substrate

The first cascades were run in three different buffer systems (TRIS-HCl, KpI, HEPES) with a pH of 7.5 and a concentration of 100 mM in a volume of 50 μL in a 1.5-mL tube at 700 rpm ThermoMixer C, Eppendorf, Germany) and 37 °C. Cascade mixtures containing cofactors, buffer and substrates were prepared in the tube and then the enzyme mixture was added. Samples were taken directly after enzyme addition and at the indicated time points. They were diluted 1 to 10 or 1 to 20 in 2.5 mM H$_2$SO$_4$ and filtered using modified PES 10 kDa (VWR) centrifugal filters.

Formaldehyde addition via micro syringe pumps

Cascades with formaldehyde titration were conducted similarly in a volume of 200 μL in a 2 mL tube applying 700 rpm (ThermoMixer C, Eppendorf, Germany) at 37 °C. Substrates (except formaldehyde), buffers and cofactors were presented in the tube and then the enzyme mixture was added. The reaction tubes were perforated and the cascade solution was connected to the formaldehyde solution through a tubing. 100 mM formaldehyde stock solution was applied directly through the tubing with a gas tight syringe (SGE) and microsyringe pump (Flowstart EVO, Future Chemistry, The Netherlands) after addition of the enzymes. The flow rate of formaldehyde was set to either 20 μL h^{-1} or 10 μL h^{-1} and the tube was sealed with parafilm. The flow rate of formaldehyde was set to 0 μL h^{-1} after five (20 μL h^{-1}) and ten hours (10 μL h^{-1}) of application. Samples over a period of 26 h (20 μL h^{-1}) or 18 h (10 μL h^{-1}) were taken and handled as described before.

Final cascade with methanol

Cascades with methanol as substrate instead of formaldehyde were conducted in a volume of 200 μL in a 2 mL tube applying 700 rpm (ThermoMixer C, Eppendorf, Germany) at 37 °C. Substrates, buffers and cofactors were presented in the tube and then the enzyme mixture was added (Table S3). In contrast to the cascades before catalase and methanol oxidase were added to the reaction mixtures. Samples over a period of 46 h (isobutanol) and 24 h (ethanol) were taken as described before.

Cascade control experiments

Control experiments were conducted similarly to the cascade experiments without the addition of methanol oxidase and transketolase (Figure S7).

Quantification of cascade substrates, intermediates and products

Quantification of methanol, acetaldehyde, isobutyraldehyde ethanol and isobutanol

Methanol, acetaldehyde, isobutyraldehyde, ethanol and isobutanol were quantified by headspace GC-FID [Thermo Scientific Trace GC Ultra, equipped with a flame ionization detector (FID) and a Headspace Tri Plus autosampler] equipped with a Stabilwax column [30 m, 0.25 mm internal diameter, 0.25 μm film thickness (Restek, Bellefonte, USA)] with helium as carrier gas similar to Guterl et al.[18] The oven temperature was held at 50 °C for 2 min and raised with

ChemSusChem

Research Article
doi.org/10.1002/cssc.202202122

Chemistry
Europe
European Chemical
Societies Publishing

10 °C min⁻¹ to 80 °C held for 1 min. 200 μL of the samples were added to a 10 mL headspace vial for analysis. Prior to injection samples were incubated at 40 °C for 15 min. Injection was carried out via split mode with 10 mL min⁻¹ flow, with an injection volume of 700 μL using headspace mode.

Quantification of xylose, xylulose, glyceraldehyde, dihydroxyacetone and pyruvate

Xylose, xylulose, glyceraldehyde, dihydroxyacetone and pyruvate were analyzed and quantified using an HPLC (Ultimate300 HPLC-system, Dionex Softron GmbH, Germaring, Germany) system coupled to an UV-detector at 210 nm and an RI detector, equipped with a Rezex™ ROA-Organic Acid H+ (8%) 300 x 7.8 mm LC Column (Phenomenex, Germany). Separation was conducted in an isocratic run with 2.5 mM H_2SO_4 at 70 °C for 42 min.[14a] Signal analysis and amount calculation was conducted by using Chromeleon Software (Thermofisher Scientific).

Quantification of formaldehyde

Formaldehyde was quantified using the acetylacetone method.[52] Therefore formaldehyde standards (1 mM, 0.8 mM, 0.4 mM, 0.2 mM, 0.1 mM, 0.05 mM, 0.01 mM and 0 mM) were prepared in the cascade mix (Table S5). 50 μL of diluted cascade samples or standards were mixed with 50 μL Nash reagent [0.2% (v v⁻¹) acetylacetone, 0.1 M acetic acid and 3.89 M ammonium acetate] in a 96 well plate and incubated for 30 min at 37 °C. Absorbance was measured at 412 nm with a Biotek epoch-2 microplate spectrophotometer (Biorad).

Conflict of Interest

All authors declare that they have no competing interests.

Data Availability Statement

The authors declare that the data supporting the findings of this study are available within the paper and its supplementary information.

Keywords: biofuels · enzyme cascade · lignocellulosic biomass · methanol · xylose

[1] R. A. Sheldon, J. M. Woodley, *Chem. Rev.* **2018**, *118*, 801–838.
[2] Y. Su, W. Zhang, A. Zhang, W. Shao, *Appl. Sci.* **2020**, *10*, 8222.
[3] S. Fatma, A. Hameed, M. Noman, T. Ahmed, M. Shahid, M. Tariq, I. Sohail, R. Tabassum, *Protein Pept. Lett.* **2018**, *25*, 148–163.
[4] S. Kwak, Y.-S. Jin, *Microb. Cell Fact.* **2017**, *16*, 82.
[5] J. Baruah, B. K. Nath, R. Sharma, S. Kumar, R. C. Deka, D. C. Baruah, E. Kalita, *Front. Energy Res.* **2018**, *6*, 141.
[6] a) A. D. Chintagunta, G. Zuccaro, M. Kumar, S. J. Kumar, V. K. Garlapati, P. D. Postemsky, N. S. Kumar, A. K. Chandel, J. Simal-Gandara, *Front. Microbiol.* **2021**, *12*, 658284; b) A. Lachke, *Reson* **2002**, *7*, 50–58.
[7] K. Cheng, W. Zheng, H. Chen, Y.-H. P. J. Zhang, *Metab. Eng.* **2019**, *52*, 1–8.
[8] a) Z. Zhao, M. Xian, M. Liu, G. Zhao, *Biotechnol. Biofuels* **2020**, *13*, 21; b) T. W. Jeffries, *Adv Biochem Eng Biotechnol.* **1983**, *27*, 1–32.
[9] a) E. M. Ammar, X. Wang, C. V. Rao, *Sci. Rep.* **2018**, *8*, 609; b) C. Van Zyl, B. A. Prior, S. G. Kilian, J. L. Kock, *Microbiology* **1989**, *135*, 2791–2798.
[10] W. Yin, Y. Cao, M. Jin, M. Xian, W. Liu, *ACS Synth. Biol.* **2021**, *10*, 2266–2275.
[11] S. G. Karp, J. D. Medina, L. A. Letti, A. L. Woiciechowski, J. C. de Carvalho, C. C. Schmitt, R. de Oliveira Penha, G. S. Kumlehn, C. R. Soccol, *Biofuels Bioprod. Biorefin.* **2021**, *15*, 899–912.
[12] S. Malakar, S. K. Paul, K. R. Jolvis Pou, in *Biotechnological Progress and Beverage Consumption* (Eds.: A. M. Grumezescu, A. M. Holban), Academic Press, **2020**, 1–37.
[13] L. Canilha, A. Kumar Chandel, T. S. dos Santos Milessi, F. A. Fernandes Antunes, W. L. da Costa Freitas, M. das Graças Almeida Felipe, S. S. da Silva, *J. Biomed. Biotechnol.* **2012**, *2012*, 989572.
[14] a) S. Sutiono, B. Teshima, B. Beer, G. Schenk, V. Sieber, *ACS Catal.* **2020**, *10*, 3110–3118; b) F. Yang, M. A. Hanna, R. Sun, *Biotechnol. Biofuels* **2012**, *5*, 13.
[15] X. Li, Y. Chen, J. Nielsen, *Curr. Opin. Biotechnol.* **2019**, *57*, 56–65.
[16] Y. Cam, C. Alkim, D. Trichez, V. Trebosc, A. Vax, F. Bartolo, P. Besse, J. M. François, T. Walther, *ACS Synth. Biol.* **2016**, *5*, 607–618.
[17] T. C. Ezeji, N. Qureshi, V. Ujor, in *Bioenergy Res.: Adv. Appl.* (Eds.: V. K. Gupta, M. G. Tuohy, C. P. Kubicek, J. Saddler, F. Xu), Elsevier, Amsterdam, **2014**, 109–118.
[18] J. K. Guterl, D. Garbe, J. Carsten, F. Steffler, B. Sommer, S. Reiße, A. Philipp, M. Haack, B. Rühmann, A. Koltermann, *ChemSusChem* **2012**, *5*, 2165–2172.
[19] a) D. Dugar, G. Stephanopoulos, *Nat. Biotechnol.* **2011**, *29*, 1074–1078; b) N. Maleki, M. Safari, M. A. Eiteman, *Eng. Life Sci.* **2018**, *18*, 40–47.
[20] S. Atsumi, T. Hanai, J. C. Liao, *Nature* **2008**, *451*, 86–89.
[21] S. Sherkhanov, T. P. Korman, S. Chan, S. Faham, H. Liu, M. R. Sawaya, W.-T. Hsu, E. Vikram, T. Cheng, J. U. Bowie, *Nat. Commun.* **2020**, *11*, 4292.
[22] P. Promdonkoy, W. Mhuantong, V. Champreda, S. Tanapongpipat, W. Runguphan, *J. Ind. Microbiol. Biotechnol.* **2020**, *47*, 497–510.
[23] a) P. Promdonkoy, W. Siripong, J. J. Downes, S. Tanapongpipat, W. Runguphan, *AMB Expr.* **2019**, *9*, 160; b) J. M. Clomburg, R. Gonzalez, *Appl. Microbiol. Biotechnol.* **2010**, *86*, 419–434; c) Y. Zhang, S. Lane, J.-M. Chen, S. K. Hammer, J. Luttinger, L. Yang, Y.-S. Jin, J. L. Avalos, *Biotechnol. Biofuels* **2019**, *12*, 223.
[24] C. Fu, Z. Li, C. Jia, W. Zhang, Y. Zhang, C. Yi, S. Xie, *Energy Convers. Manage. X* **2021**, *10*, 100059.
[25] a) X. Jia, R. M. Kelly, Y. Han, *Metab. Eng. Commun.* **2018**, *7*, e00074; b) H. Boer, M. Andberg, R. Pylkkänen, H. Maaheimo, A. Koivula, *AMB Expr.* **2019**, *9*, 48.
[26] H. Yurimoto, N. Kato, Y. Sakai, *Chem. Rec.* **2005**, *5*, 367–375.
[27] H. Yurimoto, M. Oku, Y. Sakai, *Int. J. Microbiol.* **2011**, *2011*, 101298.
[28] W. Zhang, T. Zhang, S. Wu, M. Wu, F. Xin, W. Dong, J. Ma, M. Zhang, M. Jiang, *RSC Adv.* **2017**, *7*, 4083–4091.
[29] a) C.-T. Chen, F. Y.-H. Chen, I. W. Bogorad, T.-Y. Wu, R. Zhang, A. S. Lee, J. C. Liao, *Metab. Eng.* **2018**, *49*, 257–266; b) F. Meyer, P. Keller, J. Hartl, O. G. Gröninger, P. Kiefer, J. A. Vorholt, *Nat. Commun.* **2018**, *9*, 1508.
[30] a) P. L. Bergquist, S. Siddiqui, A. Sunna, *Front. Energy Res.* **2020**, *8, 193*; b) H. J. Lim, D.-M. Kim, *Curr. Opin. Biotechnol.* **2022**, *73*, 158–163; c) N. Losada-Garcia, Z. Cabrera, P. Urrutia, C. Garcia-Sanz, A. Andreu, J. M. Palomo, *Catalysts* **2020**, *10*, 1258.
[31] T. Cai, H. Sun, J. Qiao, L. Zhu, F. Zhang, J. Zhang, Z. Tang, X. Wei, J. Yang, Q. Yuan, W. Wang, X. Yang, H. Chu, Q. Wang, C. You, H. Ma, Y. Sun, Y. Li, C. Li, H. Jiang, Q. Wang, Y. Ma, *Science* **2021**, *373*, 1523–1527.
[32] S. Atsumi, W. Higashide, J. C. Liao, *Nat. Biotechnol.* **2009**, *27*, 1177–1180.
[33] R. Miao, H. Xie, P. Lindblad, *Biotechnol. Biofuels* **2018**, *11*, 267.
[34] L. Guo, L. Sun, Y.-X. Huo, *Biotechnol. Biofuels Bioprod.* **2022**, *15*, 80.

[35] J. B. Siegel, A. L. Smith, S. Poust, A. J. Wargacki, A. Bar-Even, C. Louw, B. W. Shen, C. B. Eiben, H. M. Tran, E. Noor, *Proc. Nat. Acad. Sci.* **2015**, *112*, 3704–3709.

[36] a) K. Nobuo, H. Toshio, S. Chikahiro, N. Tsutomu, T. Yoshiki, Y. Hideaki, *Biochim. Biophys. Acta* **1982**, *715*, 143–150; b) Y. T. Ro, C. Y. Eom, T. Song, J. W. Cho, Y. M. Kim, *J. Bacteriol.* **1997**, *179*, 6041–6047; c) G. A. Sprenger, U. Schörken, G. Sprenger, H. Sahm, *Eur. J. Biochem.* **1995**, *230*, 525–532.

[37] P. H. Opgenorth, T. P. Korman, L. Iancu, J. U. Bowie, *Nat. Chem. Biol.* **2017**, *13*, 938–942.

[38] A. Pick, B. Rühmann, J. Schmid, V. Sieber, *Appl. Microbiol. Biotechnol.* **2013**, *97*, 5815–5824.

[39] G. M. Rodriguez, S. Atsumi, *Metab. Eng.* **2014**, *25*, 227–237.

[40] S. Sutiono, J. Carsten, V. Sieber, *ChemSusChem* **2018**, *11*, 3335–3344.

[41] J. Wei, J. G. Timler, C. M. Knutson, B. M. Barney, *FEMS Microbiol. Lett.* **2013**, *346*, 105–112.

[42] B. Sommer, H. von Moeller, M. Haack, F. Qoura, C. Langner, G. Bourenkov, D. Garbe, B. Loll, T. Brück, *ChemBioChem* **2015**, *16*, 110–118.

[43] R. K. Bennett, G. J. Gregory, J. E. Gonzalez, J. R. G. Har, M. R. Antoniewicz, E. T. Papoutsakis, *Front. Microbiol.* **2021**, *12*, 638426.

[44] S. Navarro-Jaén, M. Virginie, J. Bonin, M. Robert, R. Wojcieszak, A. Y. Khodakov, *Nat. Chem. Rev.* **2021**, *5*, 564–579.

[45] a) S. Chakrabortty, J. Nayak, B. Ruj, P. Pal, R. Kumar, S. Banerjee, M. Sardar, P. Chakraborty, *J. Environ. Chem. Eng.* **2020**, *8*, 103935; b) H. Guzmán, F. Salomone, E. Batuecas, T. Tommasi, N. Russo, S. Bensaid, S. Hernández, *Chem. Eng. J.* **2021**, *417*, 127973.

[46] W. R. Birmingham, A. Toftgaard Pedersen, M. Dias Gomes, M. Bøje Madsen, M. Breuer, J. M. Woodley, N. J. Turner, *Nat. Commun.* **2021**, *12*, 4946.

[47] R. Couderc, J. Baratti, *Agric. Biol. Chem.* **1980**, *44*, 2279–2289.

[48] M. Dias Gomes, B. R. Bommarius, S. R. Anderson, B. D. Feske, J. M. Woodley, A. S. Bommarius, *Adv. Synth. Catal.* **2019**, *361*, 2574–2581.

[49] F. W. Studier, *Protein Expression Purif.* **2005**, *41*, 207–234.

[50] T. J. Gmelch, J. M. Sperl, V. Sieber, *ACS Synth. Biol.* **2020**, *9*, 920–929.

[51] D. Gauss, I. Sánchez-Moreno, I. Oroz-Guinea, E. García-Junceda, R. Wohlgemuth, *Eur. J. Org. Chem.* **2018**, 2892–2895.

[52] H.-J. Jo, J.-H. Kim, Y.-N. Kim, P.-W. Seo, C.-Y. Kim, J.-W. Kim, H.-n. Yu, H. Cheon, E. Y. Lee, J.-S. Kim, *Green Chem.* **2022**, *24*, 218–226.